Available online at www.sciencedirect.com
ScienceDirect
Carbohydrate Polymers 70 (2007) 1–7
Carbohydrate Polymers
www.elsevier.com/locate/carbpol

Investigation of starch retrogradation using atomic force microscopy

Mary Chiming Tang, Les Copeland *

Faculty of Agriculture, Food and Natural Resources, University of Sydney, NSW 2006, Australia

Received 3 December 2006; received in revised form 2 February 2007; accepted 16 February 2007
Available online 1 March 2007

Abstract

The formation of molecular networks by retrogradation of gelatinised starch was investigated using atomic force microscopy in tapping mode. Specimens were prepared from wheat and maize starches that were mixed into a paste in a Rapid Visco Analyzer at 90 °C. The paste was subsequently diluted for specimen preparation. When diluted pastes from wheat starch containing 25.5% amylose and maize starch with 30.7% amylose were deposited on to a mica stage at 90 °C, an extended network structure was clearly evident. However, when monopalmitin, which forms complexes with amylose, was mixed in with the starch paste, aggregated structures were observed rather than a network. Aggregated structures were also observed in starch from waxy maize with specimens prepared at 90 °C. These results will be discussed in relation to the significance of amylose in the formation of starch gels after retrogradation.

Keywords: Starch retrogradation; Starch gel; Starch network; Starch–lipid complexes

1. Introduction

Understanding how starch is affected by processing, cooking and interactions with other molecules is of considerable interest given the importance of starch in many foods and as the main source of energy in the human diet. Starch is made up of two types of polymers of glucose: essentially unbranched amylose, and amylopectin, a larger molecule with multiple branches of differing length and distribution. Genetic and environmental influences on the biosynthesis lead to considerable variation in starches between and within plant species. These variations may be in the size and shape of starch granules, amylose, and amylopectin content, and in the branching pattern of amylopectin, all of which can affect the functional and nutritional properties of the starch.

When starch is heated with stirring in water it gelatinises into a viscoelastic paste, which on cooling retrogrades to form a semi-crystalline gel. Depending on the amylose content, most starches form firm gels on cooling, although waxy starches, which contain little or no amylose, tend to retrograde more slowly and remain as a cohesive paste (Thomas & Atwell, 1999). The presence of lipids, emulsifiers or ions can affect gelatinisation and retrogradation (Richardson, Kidman, Langton, & Hermansson, 2004; Richardson, Langton, Bark, & Hermansson, 2003; Richardson, Sun, Langton, & Hermanson, 2004; Toro-Vazquez et al., 2003). Retrograded starch gels are generally considered to contain macromolecular networks, which have been observed by transmission and scanning electron microscopy (Doublier & Choplin, 1989; Hoover & Hadziyev, 1981; Leloup & Colonna, 1992; Putaux, Buléon, & Chanzy, 2000; Richardson et al., 2004; Richardson, Sun et al., 2004). However, the mechanism of network formation is still not well understood.

The atomic force microscope (AFM) is a scanning probe microscope with resolution in the nano- to micrometer range that has been used to examine the morphology of starch granules and starch molecules (Dang & Copeland, 2003; Gunning et al., 2003; Liu, Guo, Hu, & Li, 2001; McIntire & Brant, 1999; Szymonaska & Krok, 2003). Amylose from rice and potato amylopectin have also been examined after gelatinisation and cooling; amylose was

* Corresponding author. Tel.: +61 2 9351 2935; fax: +61 2 9351 2945.
E-mail address: l.copeland@usyd.edu.au (L. Copeland).

0144-8617/$ - see front matter © 2007 Elsevier Ltd. All rights reserved.
doi:10.1016/j.carbpol.2007.02.025

observed to form highly aggregated structures after cooking and cooling (Dang, Braet, & Copeland, 2006). In this study, we have used the AFM to image the network structure of retrograded starch gels. The role of amylose in the network has been studied by examining how the gels are affected by the addition of monoglycerides to the starch, and from comparative studies with waxy starch.

2. Materials and methods

2.1. Materials

Starches were obtained from Penford Pty Ltd (Lane Cove, NSW, Australia) and were used as supplied. According to the supplier's specifications, the amylose content of the wheat starch, maize starch, and waxy maize starch was 25.5%, 30.7%, and 6.7%, respectively. The moisture content of the starch samples was approximately 10%. Monopalmitin and monostearin were from Sigma–Aldrich (St. Louis, MO, USA). Analytical grade isoamylase (EC 3.2.1.68) was from Megazyme International, Bray Ireland.

2.2. Preparation of specimens for AFM

Starch (30 mg), and monopalmitin or monostearin (0.5 mg) as indicated in the Results, were weighed into an RVA canister and 30 ml of distilled water were added. The plastic paddle was raised and lowered through the canister 10 times to mix the contents before inserting the canister into the RVA instrument (Newport Scientific Rapid Visco Analyser-4). The starch suspension was stirred initially at a speed of 960 rpm for 10 s and then the stirring speed was held constant at 160 rpm during the RVA program. The suspension was heated from 50 to 95 °C in 3 min and 42 s, held at 95 °C for 2 min and 30 s, and then at 90 °C for 3 min and 48 s. This mixture was diluted immediately after the completion of the RVA program with hot water at 90 °C to a starch concentration of 30 μg/ml.

For the preparation of specimens at 90 °C, the diluted RVA paste was kept at 90 °C with frequent stirring for 20 min before 2 μl samples (containing 60 ng of starch) were spread over an area of about 1 cm^2 on freshly cleaved mica using a preheated micropipette. For specimens prepared at 37 °C, the diluted RVA paste was cooled to 37 °C in a water bath for 10 min before 2 μl samples were deposited on to the mica. The specimens were dried immediately in a 70 °C oven and stored in a desiccator at room temperature until used for imaging, usually within one week. All samples were prepared at least in duplicate from separate RVA pastes.

2.3. AFM image analysis

Specimens were observed using a Pico SPM II (Molecular Imaging Ltd, USA) in acoustic alternating current (i.e., tapping) mode. The measurements were performed in tapping mode in air at ambient temperature and pressure using a silicon cantilever NSC14/AIBS/15 (Mikro Masch, Narva) with a force constant of 5 N/m and a resonant frequency of 160 kHz. Data were acquired by measuring the deflection and force of the cantilever, and converted to the images shown using PicoScan 5 image processing software supplied by Molecular Imaging Ltd.

3. Results

When wheat starch pastes were deposited on to mica for imaging from a solution held at 90 °C, networks that extended over a large part of the field of view were observed (Fig. 1a and b). The width and height of the strands in the network were estimated from 20 observations of at least duplicate images of the type shown in Fig. 1 to be 43.3 ± 7.5 and 0.4 ± 0.1 nm, respectively. Junction zones in the network were observed in images at higher magnification (Fig. 1c and d). Irregularly shaped structures, with diameter ranging between about 200 and 650 nm and height of 10–30 nm were noted with a frequency of about once per 2000 nm^2 (Fig. 1a and b). These were assumed from their dimensions to be remnants of incompletely gelatinised starch granules, as also observed in scanning electron microscopy studies of wheat starch (Richardson, Sun et al., 2004).

Starch networks covering a large area of the mica were also clearly evident in pastes of maize starch (with 30.7% amylose) prepared at 90 °C by the same method as for wheat starch (Fig. 2a). The width and height dimensions of the strands in the network, 43.2 ± 10.1 and 0.20 ± 0.04 nm ($n = 20$), respectively, were similar to those shown for wheat starch in Fig. 1. Rounded structures with diameter of 65.2 ± 14.2 nm and height of 0.43 ± 0.18 nm ($n = 20$) were also observed (Fig. 2a). In contrast, networks were not observed with waxy maize starch prepared at 90 °C (Fig. 2b). Instead, rounded structures with diameter of 60.9 ± 10.6 nm and height of 0.6 ± 0.3 nm ($n = 20$) were abundant.

Networks were not observed in samples of wheat starch that were mixed with monopalmitin or monostearin in the RVA and deposited on to mica from a 90 °C solution (Fig. 3). Starch–monopalmitin mixtures gave round structures, with an average diameter of 33.9 ± 6.5 nm and height of 0.9 ± 0.2 nm ($n = 20$), whereas the structures observed with starch–monostearin mixtures were more elongated, with length ranging between 25 and 170 nm, and average width and height of 25.2 ± 7.7 and 2.8 ± 1.9 nm ($n = 20$), respectively. The structures in the starch–monoglyceride pastes were distributed evenly on the mica, with an average frequency of distribution of 9.1 per 200 nm^2 (SD = 1.3) for starch–monopalmitin and 8.3 per 200 nm^2 (SD = 2.2) for starch–monostearin, as measured over 10 fields of view.

When wheat starch was dispersed at 90 °C and cooled to 37 °C before the specimens were deposited on to mica for imaging, discrete rod-shaped structures were observed with average dimensions of 52.1 ± 12.4 nm in length, 35.2 ± 6.3 nm in width and 0.9 ± 0.5 nm in height

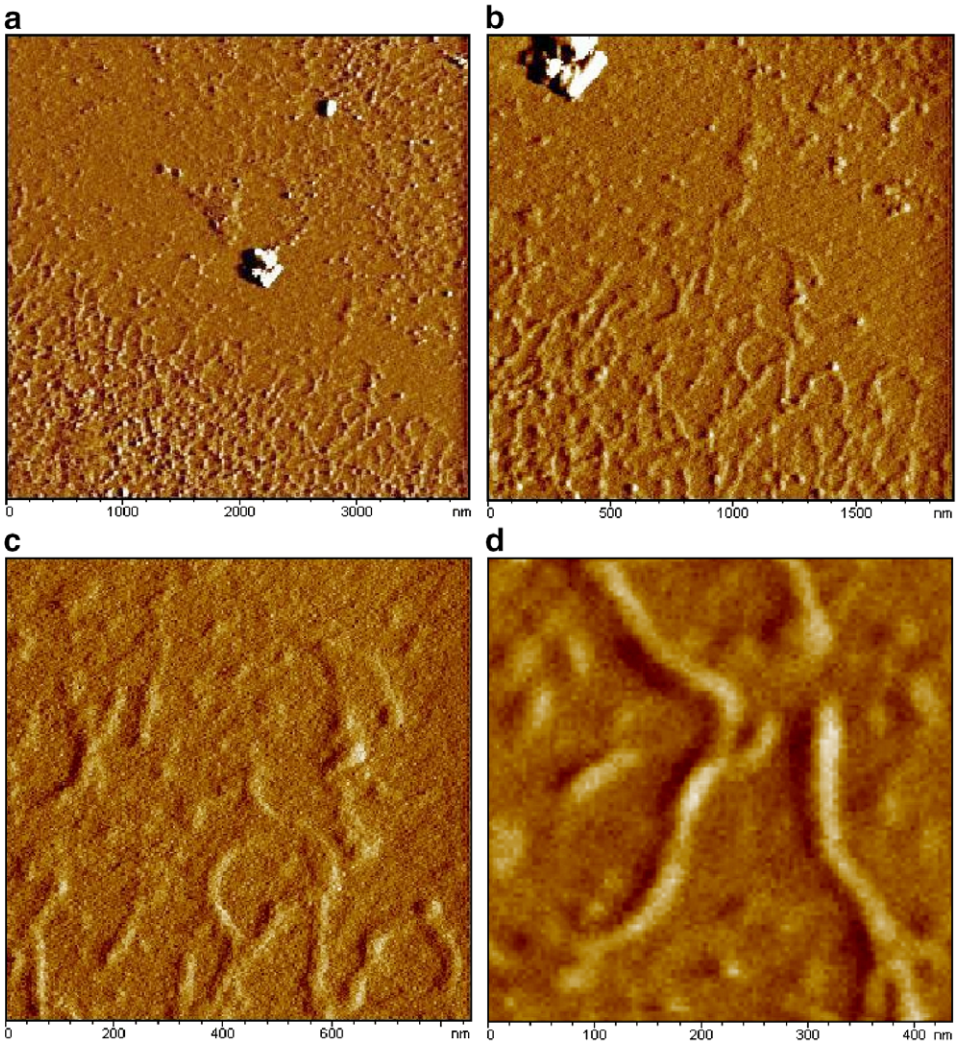

Fig. 1. AFM images of wheat starch. Starch was pasted in the RVA and 60 ng deposited on to mica from a solution kept at 90 °C, as described. The areas scanned were 4000 × 4000 nm (a), 2000 × 2000 nm (b), 830 × 830 nm (c), and 440 × 440 nm (d).

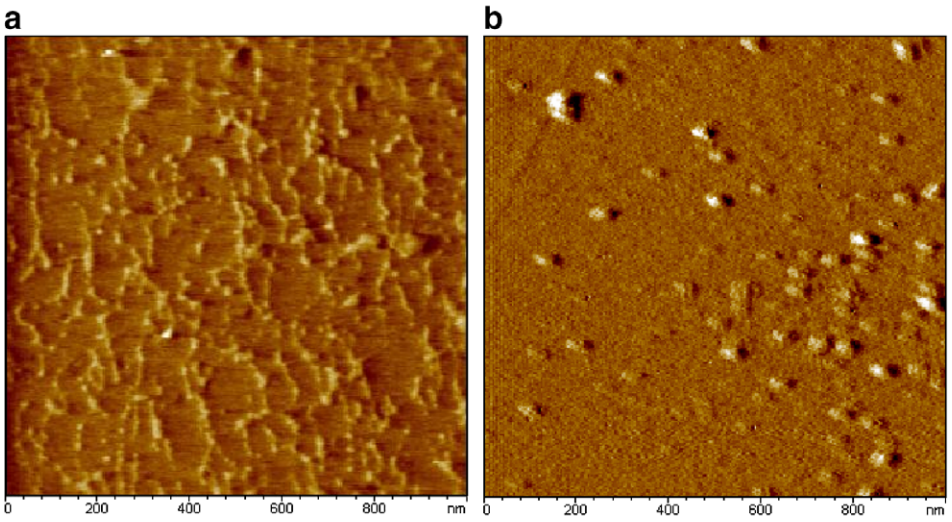

Fig. 2. AFM image of maize starch containing 30.7% amylose (a) and waxy maize starch with 6.7% amylose (b). The starches were pasted in the RVA and 60 ng deposited on to mica from a solution kept at 90 °C, as described. The areas scanned were 1000 × 1000 nm for both of (a) and (b).

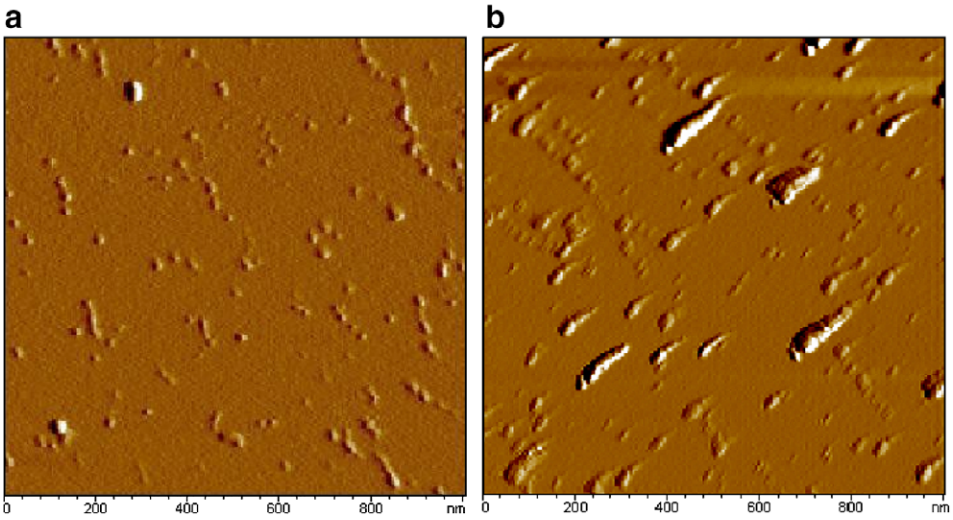

Fig. 3. AFM images of starch–lipid aggregates formed by mixing wheat starch mixed with monopalmitin (a), and wheat starch mixed with monostearin (b). Wheat starch was pasted in the RVA in present of added lipids and 60 ng deposited on to mica from a solution kept at 90 °C, as described. The areas scanned were 1000×1000 nm for both (a) and (b).

($n = 20$) (Fig. 4). Larger structures with diameter of 100–350 nm were observed occasionally. Starch–monoglyceride pastes that were prepared with monopalmitin or monostearin and cooled to 37 °C before deposition on to mica, revealed round structures with diameter between 20 and 60 nm and height of 0.5–1 nm (Fig. 5). Much larger, irregularly shaped aggregates, with diameter between about 100 and 500 nm and height of 1–20 nm, were also observed with a frequency of distribution of between one and three structures per 1000 nm^2 (Fig. 5).

Starch pastes prepared in the RVA were also inspected visually after cooling to room temperature for 30 min in the canister. With starch alone and starch mixed with tripalmitin, which does not form complexes with starch (Tang & Copeland, 2007), firm gels were observed (Fig. 6a and c). In comparison, a much softer gel was obtained when starch was mixed with monopalmitin (Fig. 6b), whereas a very runny paste was observed after isoamylase was added to the starch gel at the completion of the RVA profile (Fig. 6d). Starch pastes after treatment with isoamylase were observed under the AFM to contain multiple structures approximately 46.4 ± 9.0 nm in diameter and 0.7 ± 0.3 nm in height ($n = 20$), which were scattered evenly across the field of view (Fig. 7). Occasional larger structures were also observed, which are suggested to be due to the isoamylase. AFM images of isoamylase alone contained large structures (about 30–350 nm in diameter and 2–60 nm in height), which may represent aggregates of the enzyme produced during specimen preparation in the absence of the starch paste (Fig. 7).

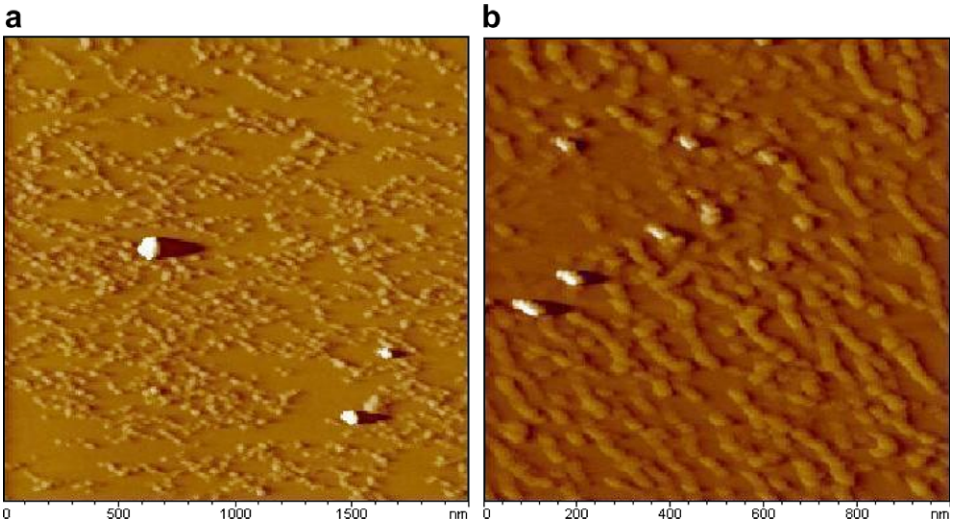

Fig. 4. AFM images of wheat starch deposited on mica from a starch solution at 37 °C. Wheat starch was pasted in the RVA, diluted at 90 °C, and the solution cooled to 37 °C before specimens (60 ng) were deposited on to mica. The areas scanned were 2000×2000 nm (a) and 1000×1000 nm (b).

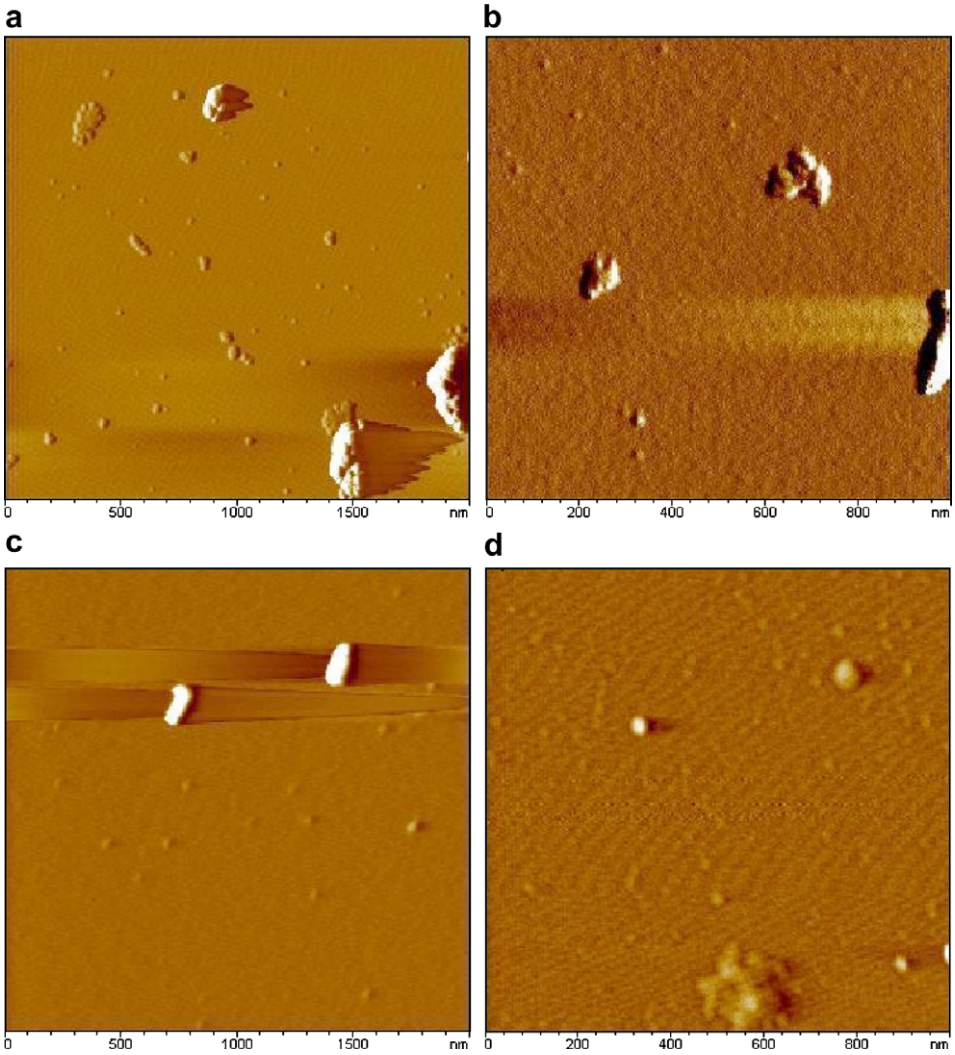

Fig. 5. AFM images of starch–monopalmitin aggregates (a,b) and starch–monostearin aggregates (c,d) in starch pastes cooled to 37 °C. Wheat starch was pasted in the RVA in the presence of added lipids as described. Starch–lipid mixtures have been cooled from 90 to 37 °C before depositing on to mica. The areas scanned were 2000 × 2000 nm (a,c) and 1000 × 1000 nm (b,d).

4. Discussion

RVA pastes were prepared from wheat starch containing 25.5% amylose and maize starch with 30.7% amylose. These pastes, which were diluted and kept at 90 °C to minimise retrogradation before deposition on to the mica, clearly showed extensive networks in AFM images. Although dilution may have altered the nature of the starch gel that had formed in the RVA, the images are likely to represent the entanglement of starch chains in the solution, since the height of the structures observed (0.2–0.4 nm) is consistent with strands that have an elevation equivalent to a single starch molecule. In comparison, starch pastes of the same concentration that had been cooled to allow partial retrogradation to take place before preparing specimens for imaging, formed networks that were much more limited and appeared more like closely aligned aggregates. The increased height and greater variability of the structures observed after cooling (compare Figs. 2 and 4) indicates that aggregation of starch chains occurred before they were adsorbed on to the mica. Networks were not observed in images of waxy maize starch, nor with wheat starch that was mixed with monoglycerides to form complexes between the lipid and amylose. The absence of networks in these specimens may mean that there is little chain entanglement in solutions of starch that does not have amylose or when the amylose is complexed with lipids. The scope for intermolecular interactions between the semi-crystalline clusters of amylopectin blocklets may be limited. The formation of larger aggregates after starch–lipid pastes were cooled may be related to the reduced solubility and fluidity of the lipid molecules at 37 °C compared to 90 °C.

The firmness of the resulting starch gels seemed to reflect the extent of the network that formed on retrogradation. The gels with starch alone, in which there were extensive networks with numerous junction zones, were firm and could be cut without collapsing. Similarly, pastes of starch mixed with tripalmitin, which does not form complexes

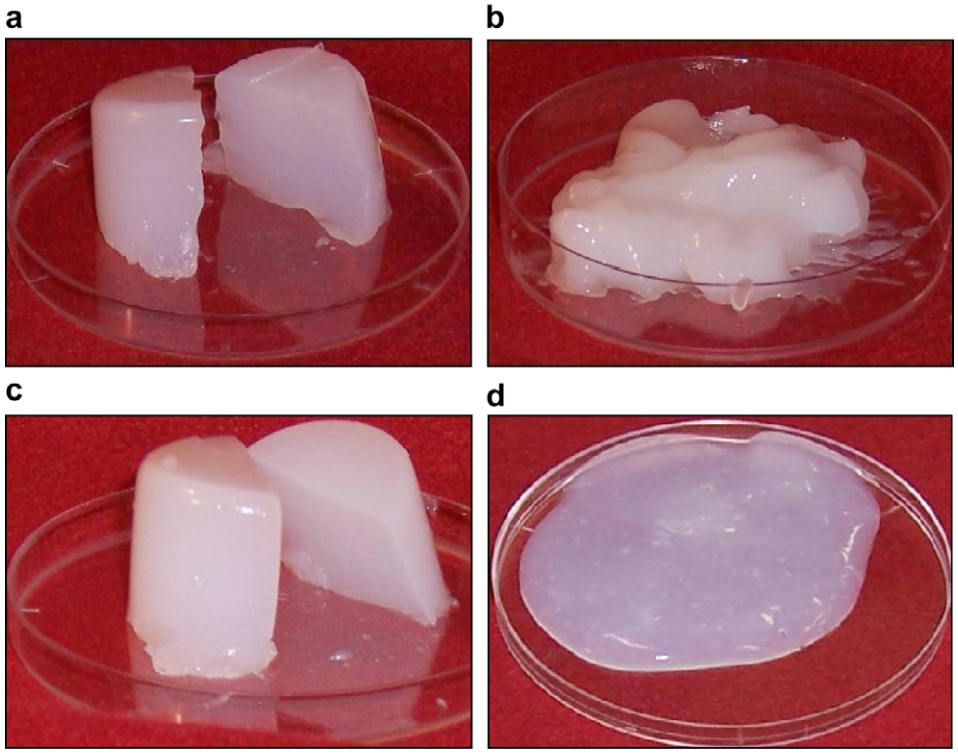

Fig. 6. Wheat starch gels prepared in the RVA from starch (a), starch mixed with monopalmitin (b), starch mixed with tripalmitin (c), and starch mixed with isoamylase (d). Wheat starch was pasted in the RVA as described in Tang and Copeland (2007), after which the pastes were kept in the RVA canister at room temperature for 30 min. Isoamylase was added to (d) immediately after the completion of the RVA protocol.

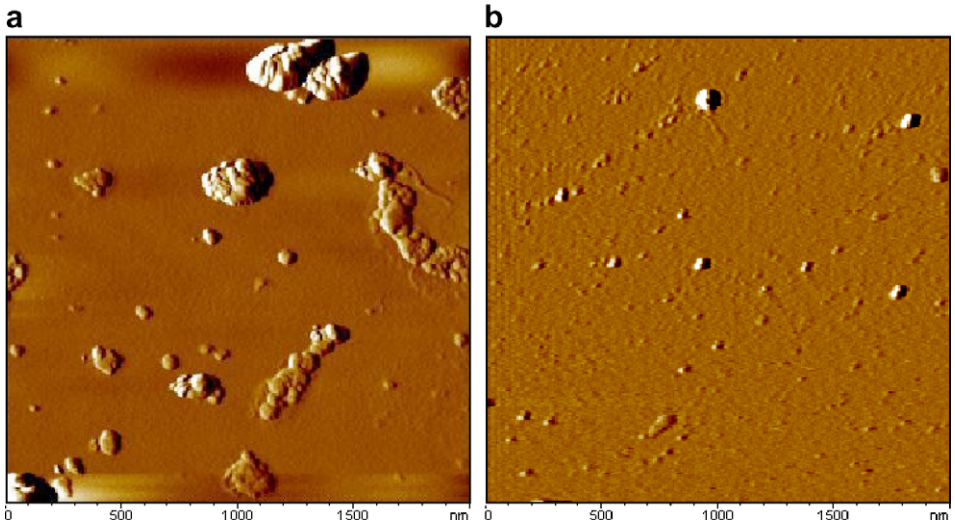

Fig. 7. AFM images of isoamylase only (a) and starch mixed with isoamylase (b). Wheat starch was pasted in the RVA as described and isoamylase mixed with starch paste after the completion of the RVA program. This mixture was incubated at 50 °C for 10 min and diluted with distilled water at 50 °C to a starch concentration of 30 μg/ml before depositing on to mica. Isoamylase (50 μl) was diluted with distilled water using the same conditions before depositing on to mica. The areas scanned were 2000×2000 nm.

with starch (Tang & Copeland, 2007), were also firm. In contrast, gels formed from starch complexed with monoglycerides, in which there were no networks, were very soft. A conclusion drawn from these results is that amylose has a key role in the formation of molecular networks in retrograded starch. This role is likely to be related to the ability of amylose molecules to link together by the formation of double helices (Jane & Robyt, 1984; Leloup & Colonna, 1992). Networks did not form in the absence of amylose (i.e., with waxy starch), or when amylose had reduced capacity to form double helices through complexation with lipids. Pastes in which the amylopectin was debranched with isoamylase formed a very soft and runny gel that did not contain a molecular network.

The strands in the network of the starch gels imaged in the present study were approximately 43 nm wide. In comparison, the width of a single amylose chain has been estimated to be 0.54 nm (McIntire & Brant, 1999), whereas gelatinised and cooled amylose from rice starch formed aggregates, proposed to contain multiple chains, which were observed with the AFM to be 6–19 nm in width (Dang et al., 2006). Uncooked, native rice grains imaged directly by AFM showed structures approximately 100 nm in width, which were suggested to represent amylopectin chain clusters in starch crystallites (Dang & Copeland, 2003). On the basis of these different observations, it seems reasonable to propose that the starch networks observed in the present study were made up of aggregates of both amylose and amylopectin molecules. Pea starch gels, which were prepared in a way so as to not disrupt the granule structure, were proposed to be composites of gelatinised starch granules trapped in an amylose matrix (Miles, Morris, Orford, & Ring, 1985). However, in the present study, there was a low frequency of undisrupted granules due to the vigorous mixing in the RVA. Whether the gels are made up of amylopectin molecules trapped in a matrix of aggregated amylose chains, or whether there are double helical interactions between amylose and external branches of amylopectin, as has been suggested to occur in starch blocklets within granules (Tang, Mitsunaga, & Kawamura, 2006), would be of interest in further studies.

Acknowledgements

MCT was supported by a scholarship from the Value Added Wheat CRC Pty Ltd. The authors are grateful to Newport Scientific for making available an RVA-4 instrument, and to Penford Australia Pty Ltd. for providing the wheat starch. The authors thank David Saxey, Adam Sikorski and Pall Thordarson of the University of Sydney's Electron Microscope Unit for assistance with the atomic force microscope.

References

Dang, J. M. C., Braet, F., & Copeland, L. (2006). Nanostructural analysis of starch components by atomic force microscopy. *Journal of Microscopy, 224*, 181–186.

Dang, J. M. C., & Copeland, L. (2003). Imaging rice grains using atomic force microscopy. *Journal of Cereal Science, 37*, 165–170.

Doublier, J. –L., & Choplin, L. (1989). A rheological description of amylose gelation. *Carbohydrate Research, 193*, 215–226.

Gunning, A. P., Giardina, T. P., Faulds, C. B., Juge, N., Ring, S. G., Williamson, G., et al. (2003). Surfactant-mediated solubilization of amylose and visualisation by atomic force microscopy. *Carbohydrate Polymers, 51*, 177–182.

Hoover, R., & Hadziyev, D. (1981). Characterization of potato starch and its monoglyceride complexes. *Starch/Stärke, 33*, 290–300.

Jane, J. L., & Robyt, J. F. (1984). Structure studies of amylose – V complexes and retrograded amylose by action of alpha amylases, and a new method for preparing amylodexitrins. *Carbohydrate Research, 132*, 105–118.

Leloup, V. M., & Colonna, P. (1992). Microstructure of amylose gels. *Carbohydrate Polymers, 18*, 189–197.

Liu, Z., Guo, Y., Hu, J., & Li, M. (2001). Study on the chain structure of starch molecules by atomic force microscopy. *Journal of Vacuum Science and Technology B, 19*, 111–114.

McIntire, T. M., & Brant, D. A. (1999). Imaging of carrageenan macrocycles and amylose using noncontact atomic force microscopy. *International Journal of Biological Macromolecules, 26*, 303–310.

Miles, M. J., Morris, V. J., Orford, P. D., & Ring, S. G. (1985). The roles of amylose and amylopectin in the gelation and retrogradation of starch. *Carbohydrate Research, 135*, 271–281.

Putaux, J. L., Buléon, A., & Chanzy, H. (2000). Network formation in dilute amylose and amylopectin studied by TEM. *Macromolecules, 33*, 6416–6422.

Richardson, G., Kidman, S., Langton, M., & Hermansson, A. M. (2004). Differences in amylose aggregation and starch gel formation with emulsifiers. *Carbohydrate Polymers, 58*, 7–13.

Richardson, G., Langton, M., Bark, A., & Hermansson, A. M. (2003). Wheat starch gelatinisation – the effects of sucrose, emulsifier and the physical state of the emulsifier. *Starch/Stärke, 55*, 150–161.

Richardson, G., Sun, Y., Langton, M., & Hermanson, A. M. (2004). Effect of Ca- and Na-lignosulfonate on starch gelatinisation and network formation. *Carbohydrate Polymers, 57*, 367–377.

Szymonaska, J., & Krok, F. (2003). Potato starch granule nanostructure studied by high resolution non-contact AFM. *International Journal of Biological Macromolecules, 33*, 1–7.

Tang, M. C., & Copeland, L. (2007). Analysis of complexes between lipids and wheat starch. *Carbohydrate Polymers, 67*, 80–85.

Tang, H., Mitsunaga, T., & Kawamura, Y. (2006). Molecular arrangement in blocklets and starch granule architecture. *Carbohydrate Polymers, 63*, 555–560.

Thomas, D. J., & Atwell, W. A. (1999). Starch structure. In D. J. Thomas & W. A. Atwell (Eds.), *Starches* (pp. 1–12). Eagan Press.

Toro-Vazquez, J. F., Gómez-Aldapa, C. A., Aragon-Piña, A., Fuente, E. B. L., Dibildox-Alvarado, E., & Charó-Alonso, M. (2003). Interaction of granular maize starch with lysophosphatidylcholine evaluated by calorimetry, mechanical and microscopy analysis. *Journal of Cereal Science, 38*, 269–279.